1,2,4-Triazolo[4,3-*a*]quinoxalin-1-one Moiety as an Attractive Scaffold To Develop New Potent and Selective Human A_3 Adenosine Receptor Antagonists: Synthesis, Pharmacological, and Ligand−Receptor Modeling Studies

Vittoria Colotta,*,† Daniela Catarzi,† Flavia Varano,† Francesca Romana Calabri,† Ombretta Lenzi,† Guido Filacchioni,† Claudia Martini,‡ Letizia Trincavelli,‡ Francesca Deflorian,§ and Stefano Moro§

Dipartimento di Scienze Farmaceutiche, Università degli Studi di Firenze, Polo Scientifico, Via Ugo Schiff, 6, 50019 Sesto Fiorentino (FI), Italy, Dipartimento di Psichiatria, Neurobiologia, Farmacologia e Biotecnologie, Università degli Studi di Pisa, Via Bonanno, 6, 50126 Pisa, Italy, and Molecular Modeling Section, Dipartimento di Scienze Farmaceutiche, Università degli Studi di Padova, Via Marzolo, 5, 35131 Padova, Italy

Received December 12, 2003

In the past few years much effort in our laboratory has been directed toward the study of adenosine receptor antagonists, and recently we focused our attention on 2-aryl-1,2,4-triazolo-[4,3-*a*]quinoxaline-1,4-diones and 2-aryl-1,2,4-triazolo[4,3-*a*]quinoxalin-4-amino-1-ones, some of which were potent and/or selective A_3 receptor antagonists. In the present paper, a new series of triazoloquinoxaline derivatives is described. Most of the new compounds, biologically evaluated in radioligand binding assays at bovine (b) A_1 and A_{2A} and at human (h) A_1 and A_3 adenosine receptors, showed high hA_3 adenosine receptor affinity and selectivity. In particular, 2-(4-nitrophenyl)-1,2,4,5-tetrahydro-1,2,4-triazolo[4,3-*a*]quinoxaline-1,4-dione (**1**), also tested at the hA_{2A} ARs, shows the best binding profile with a high hA_3 affinity (K_i = 0.60 nM) and strong selectivity vs hA_1 and vs hA_{2A} receptors (both selectivity ratios greater than 16 600). To interpret our experimental results, we decided to theoretically depict the putative transmembrane binding motif of our triazoloquinoxaline analogues on hA_3 receptor. Structure−activity relationships have been explained analyzing the three-dimensional structure of the antagonist−receptor models obtained by molecular docking simulation.

Introduction

The neuromodulator adenosine exerts many biological functions by activation of G-protein-coupled receptors (GPCRs), currently classified into A_1, A_{2A}, A_{2B}, and A_3 subtypes.[1,2] All four adenosine receptor (AR) subtypes have been characterized on a pharmacological level and cloned. While A_1 or A_{2A} receptors from different species show high amino acid sequence homology (85−95%), the A_3 subtype exhibits only 74% homology sequence between rat and human or sheep.[3,4] Activation of the A_3 AR subtype has been shown to mediate adenylate cyclase inhibition[5] and phospholipase C[6] and D[7] stimulation. Moreover, in a rat model it has been demonstrated that activation of A_3 ARs causes the release of inflammatory and allergic mediators from mast cells.[8] On this basis, A_3 AR antagonists might be useful as antiinflammatory and antiasthmatic agents.[9] Moreover, the A_3 AR subtype seems to be involved in cell survival regulation.[10] This makes A_3 AR antagonists promising therapeutics in counteracting ischemia- and aging-associated neurodegeneration.[10,11]

In the past few years much effort in our laboratory has been directed toward the study of AR antagonists,[12−15] and recently we focused our attention on 2-aryl-1,2,4-triazolo[4,3-*a*]quinoxaline-1,4-diones and 2-aryl-1,2,4-triazolo[4,3-*a*]quinoxalin-4-amino-1-ones (Chart 1), some of which were potent and/or selective A_3 AR antagonists.[16,17] In this class of compounds the influence of various substituents on different regions of the triazoloquinoxaline framework, i.e., the appended 2-phenyl ring or the benzofused moiety, was evaluated. The SAR studies indicated that a *p*-methoxy group on the 2-phenyl ring (compounds **1A** and **1B**)[16] as well as a 6-nitro substituent (compound **2B**)[17] shifted the affinity toward the A_3 AR subtype. Thus, taking **1A**, **1B**, and **2B** as lead compounds, we rationally designed new 1,2,4-triazolo-[4,3-*a*]quinoxaline derivatives, either 1,4-dioxo (compounds **1**−**12**, series **A**) or 4-amino-1-oxo substituted (compounds **13**−**21**, series **B**) (Chart 2), with the purpose of increasing the A_3 AR affinity and/or A_3 vs A_1 selectivity of the leads. First, we replaced the 2-(4-methoxyphenyl) substituent of compounds **1A** and **1B** with simple substituents (compounds **1**−**6** and **13**−**16**), most of which possess electronic properties similar to those of the methoxy group (amino, dimethylamino, ethoxy, and hydroxy groups) (Table 1). In the second phase of the work, the substituents on the 2-phenyl ring, which were profitable for A_3 affinity and/or A_3 vs A_1

Chart 1. Previously Reported 1,2,4-Triazolo[4,3-*a*]quinoxaline Derivatives

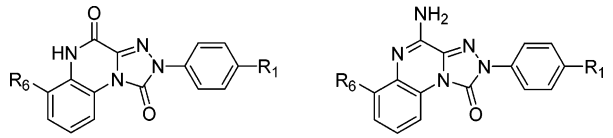

1A R_1=OMe R_6=H

1B R_1=OMe R_6=H
2B R_1=H R_6=NO_2

* To whom correspondence should be addressed. Phone: +39 55 4573731. Fax: +39 55 4573780. E-mail: vittoria.colotta@unifi.it.
† Università degli Studi di Firenze.
‡ Università degli Studi di Pisa.
§ Università degli Studi di Padova.

10.1021/jm031136l CCC: $27.50
Published on Web 06/04/2004

Chart 2. Currently Reported 1,2,4-Triazolo[4,3-*a*]quinoxaline Derivatives

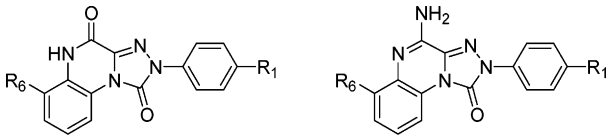

selectivity in both the present (R_1 = OH, $OCOCH_3$, NO_2) and previous studies[16,17] (R_1 = OMe), were variously combined with the 6-nitro group (compounds **7**−**10** and **17**−**19**) in order to verify whether the positive effects of these groups on hA_3 AR affinity and/or selectivity were additive. Finally, the 6-nitro derivatives **8**, **9**, **18**, and **19** were transformed into the corresponding 6-amino derivatives **11**, **12**, **20**, and **21**.

Chemistry

The triazoloquinoxalines **1**−**21** were prepared as depicted in Schemes 1−3. Scheme 1 shows the synthesis of the 2-aryl-1,2,4,5-tetrahydro-1,2,4-triazolo[4,3-*a*]quinoxaline-1,4-diones **1**−**12**. Compounds **4**, **7**, **8** were prepared following the synthetic procedure previously reported to obtain compounds **1**[18] and **1A**[16,18] (Scheme 1). Briefly, reaction of 1,2-phenylenediamine with ethyl N^1-arylhydrazono-N^2-chloroacetates **22**,[19] **23**,[20] and **24**[21] afforded the 3-arylhydrazono-1,2,3,4-tetrahydroquinoxalin-2-ones **25**,[18] **26**, and **27**,[16,18] respectively. When the commercially available 3-nitro-1,2-phenylenediamine was reacted with the ethyl N^1-arylhydrazono-N^2-chloroacetates **22** and **24**, the 3-arylhydrazono-1,2,3,4-tetrahydro-8-nitroquinoxalin-2-ones **28** and **29** were obtained, respectively. The 8-nitro structure of compounds **28** and **29** was assigned on the basis of the ^{1}H NMR spectra of the corresponding tricyclic derivatives **7** and **8** obtained by cyclizing **28** and **29** with triphosgene. The key tool was the signal of the H-9 proton, which is easily detected, since in this class of tricyclic derivatives,[16−18] the H-9 is, in general, the most deshielded aromatic proton (about 8.6−9.4 ppm) because of the paramagnetic effect of the 1-carbonyl group. Thus, the presence in the ^{1}H NMR spectra of the triazoloquinoxalines **7** and **8** of a doublet at 8.99 and 9.02 ppm, respectively, assigned to the H-9 proton indicated that **7** and **8** were 6-nitro-substituted, and consequently, the corresponding bicyclic derivatives **28** and **29** were 8-nitro-substituted compounds. The triazolo[4,3-*a*]quinoxaline-1,4-dione **4** was prepared as above cited for **7** and **8**, i.e., by cyclizing compound **26** with triphosgene following a reported procedure[16,18] to obtain compounds **1** and **1A** from **25** and **27**, respectively. The 2-(4-aminophenyl) derivative **2** was obtained from the corresponding nitro compound **1** as described in ref 18. When compound **2** reacted with formaldehyde and sodium cyanoborohydride, the 2-(4-dimethylaminophenyl) derivative **3** was obtained. The 2-(4-hydroxyphenyl) derivative **5**[18] ensued from treatment of the 2-(4-methoxyphenyl) derivative **1A** with 48% HBr, as previously described.[18] Reaction of compound **5** with acetyl chloride gave rise to the 2-(4-acetoxyphenyl)-substituted triazoloquinoxaline **6**. Demethylation of the 2-(4-methoxyphenyl) derivative **8** afforded the corresponding 2-(4-hydroxyphenyl) derivative **9**. The 2-(4-acetoxyphenyl) derivative **10** was obtained from compound **9** and acetyl chloride. Catalytic reduction of compounds **8** and **9** yielded the corresponding 6-amino derivatives **11** and **12**.

By reaction of the triazoloquinoxaline-1,4-diones **1**, **4**, **1A**, **7**, **8**, **10** with phosphorus pentachloride and phosphorus oxychloride, the unstable 2-aryl-4-chloro-1,2,4-triazolo[4,3-*a*]quinoxalin-1-ones **30**, **31**, **32**,[16] **33**−**35** were isolated (Scheme 2). Reaction of the 4-chloro derivatives **30**−**34** with ammonia yielded the corresponding 4-amino-2-aryl-1,2-dihydro-1,2,4-triazolo[4,3-*a*]quinoxalin-1-ones **13**, **15**, **1B**,[16] **17**, **18**, while from the 4-chloro derivative **35** the 4-amino-2-(4-hydroxyphenyl)-substituted compound **19** was obtained. The nitro derivative **13** was catalytically reduced to afford the corresponding amino compound **14**. The 2-(4-hydroxyphenyl)-substituted compound **16** ensued from demethylation of the 2-(4-methoxyphenyl) derivative **1B**. Catalytic reduction of the 6-nitrotriazoloquinoxaline **18** gave the 6-amino derivative **20** (Scheme 3), which by treatment with boron tribromide yielded the 2-(4-hydroxyphenyl) compound **21**.

Biochemistry

Compounds **1**−**21** were tested for their ability to displace [^{3}H]-N^6-cyclohexyladenosine ([^{3}H]CHA) from A_1 AR in bovine cerebral cortical membranes, [^{3}H]-2-[4-(2-carboxyethyl)phenethyl]amino-5′-(*N*-ethylcarbamoyl)adenosine ([^{3}H]CGS 21680) from A_{2A} AR in bovine striatal membranes, and [^{125}I]-N^6-(4-amino-3-iodobenzyl)-5′-(*N*-methylcarbamoyl)adenosine ([^{125}I]AB-MECA) from cloned hA_3 receptor stably expressed in Chinese hamster ovary (CHO) cells. In fact, because of the high species differences in the A_3 primary amino acid sequence,[4,22,23] we tested our A_3 AR ligands on cloned hA_3 receptors.

Subsequently, we selected compounds **1**, **5**, **6**, **8**, **18**, and **20**, which showed high A_3 AR affinity (K_i < 50 nM), and the previously reported **1A** and **1B**, and we tested them for their ability to displace [^{3}H]CHA from cloned hA_1 AR in order to establish their A_3 vs A_1 selectivity within the same species. The binding results of **1**−**21**, together with those of compounds **1A**, **1B**, **2B** as comparison, are shown in Table 1. Moreover, the binding data of theophylline and 1,3-dipropyl-8-cyclopentylxanthine (DPCPX), included as antagonist reference compounds, are also reported. Compound **1**, the most potent and selective A_3 AR ligand among the herein reported compounds, was also tested for its ability to displace [^{3}H]-5′-(*N*-ethylcarboxamido)adenosine ([^{3}H]-NECA) from cloned hA_{2A} ARs. Finally, to evaluate its intrinsic activity, derivative **1** was tested for its ability to inhibit the NECA-stimulated guanosine 5′-*O*-(3-[^{35}S]-thio)triphosphate ([^{35}S]GTPγS) binding (Figure 1) in membranes prepared from CHO cells stably expressing hA_3 ARs. The [^{35}S]GTPγS binding assay is a functional model where the intrinsic activity of a ligand acting at GPCRs, including ARs,[24,25] is measured by evaluating its influence on [^{35}S]GTPγS binding to cell membranes. Agonists increase the [^{35}S]GTPγS binding because they stimulate the GDP−GTP exchange. Antagonists reduce the agonist-stimulated [^{35}S]GTPγS binding.

Table 1. Binding Activity at Bovine A_1 and A_{2A} and Human A_1 and A_3 ARs

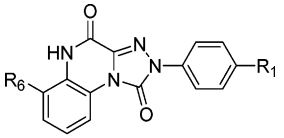

1A, 1-12

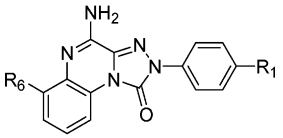

1B, 2B,13-21

			K_i [a] (nM) or I (%)			
	R_1	R_6	bA_1 [b]	hA_1 [c]	bA_{2A} [d]	hA_3 [e]
1A[e]	OMe	H	934 ± 85	42%	0%	16 ± 1.2
1	NO_2	H	19%	32%	21%	0.6 ± 0.03
2	NH_2	H	8.7 ± 0.65		28%	3600 ± 264
3	NMe_2	H	577.7 ± 48		0%	429 ± 35.9
4	OEt	H	10000 ± 866		0%	175 ± 15.3
5	OH	H	30.6 ± 2.7	168 ± 11.4	6800 ± 522	47 ± 3.9
6	OCOMe	H	26 ± 1.9	320 ± 29	9700 ± 752	11.2 ± 1.4
7	NO_2	NO_2	91 ± 7.4		0%	24%
8	OMe	NO_2	25%	0%	14%	4.7 ± 0.52
9	OH	NO_2	38%		4%	21%
10	OCOMe	NO_2	21.3%		0%	20%
11	OMe	NH_2	16%		23%	83 ± 7.4
12	OH	NH_2	996 ± 56		36%	39%
1B[f]	OMe	H	312 ± 27	69 ± 5.2	376 ± 30	45 ± 1.2
2B[g]	H	NO_2	82 ± 7.4	870 ± 22	75.8 ± 6.9	4.75 ± 0.3
13	NO_2	H	11.9%		31%	28%
14	NH_2	H	48 ± 3.9		3.6 ± 0.23	335 ± 24.9
15	OEt	H	537 ± 44		13000 ± 1240	203 ± 19.9
16	OH	H	116 ± 10.7		80 ± 7.5	73.2 ± 6.9
17	NO_2	NO_2	155 ± 13.2		2.7%	30%
18	OMe	NO_2	19%	45%	16.5%	47 ± 3.9
19	OH	NO_2	446 ± 35		1600 ± 128	45%
20	OMe	NH_2	38%	186 ± 11.3	1049 ± 98.6	22 ± 1.9
21	OH	NH_2	61 ± 5.4		181 ± 15.7	176 ± 15.9
theophylline			3800 ± 340	6200 ± 530	21000 ± 1800	86000 ± 7800
DPCPX			0.5 ± 0.03	3.2 ± 0.2	337 ± 28	1300 ± 125

[a] The K_i values are the mean ± SEM of four separate assays, each performed in triplicate. [b] Displacement of specific [^{3}H]CHA binding in bovine brain membranes or percentage of inhibition (I %) of specific binding at 20 μM concentration. [c] Displacement of specific [^{3}H]CHA binding at hA_1 receptors expressed in CHO cells or percentage of inhibition (I %) of specific binding at 10 μM concentration. [d] Displacement of specific [^{3}H]CGS 21680 binding from bovine striatal membranes or percentage of inhibition (I %) of specific binding at 20 μM concentration. [e] Displacement of specific [^{125}I]AB-MECA binding at hA_3 receptors expressed in CHO cells or percentage of inhibition (I %) of specific binding at 1 μM concentration. [f] bA_1, bA_{2A}, and hA_3 binding data are reported in ref 16. [g] Reference 17.

Results and Discussion

The binding results of compounds **1**−**21** displayed in Table 1 show that we have achieved our goal. In fact, we have produced some potent and/or highly selective hA_3 antagonists, some of which possess either increased A_3 AR affinity or hA_3 vs hA_1 selectivity with respect to those of the corresponding lead compounds (compare compounds **1** and **8** with **1A**, compound **18** with **1B**/**2B**, and derivative **20** with **1B**). Moreover, we have also obtained some potent bA_1 AR antagonists (compounds **2**, **5**, **6**, **14**, and **21**), while as expected, all the synthesized compounds except three (derivatives **14**, **16**, and **21**) are scarcely active or completely inactive at the bA_{2A} AR subtype.

The first modification we made on the lead compounds **1A** and **1B** was replacement of the *p*-methoxy group on the 2-phenyl ring with simple substituents in order to explore this position in further detail. All the substituents, but two (NO_2, OCOMe) were chosen because they possess electronic properties similar to those of the methoxy group but with different lipophilicity, steric hindrance, and above all, different ability to engage hydrogen bonds. Among the probed substituents, the *p*-nitro group on the 2-phenyl-1,2,4-triazolo[4,3-*a*]quinoxaline-1,4-dione core (compound **1**) achieved the highest A_3 affinity (K_i = 0.6 nM) among the herein reported antagonists. Compound **1** is also highly hA_3 vs hA_1 selective, being inactive at the hA_1 receptor, similar to the lead compound **1A**. To also assess the A_3 vs A_{2A} selectivity, we tested derivative **1** at the hA_{2A} ARs, toward which it is completely inactive (I = 15% at 10 μM). It is noted that **1** is among the most potent and selective hA_3 vs hA_1 and hA_3 vs hA_{2A} (both selectivity ratios greater than 16 600) tricyclic AR ligands reported so far.[26] Compound **1** resulted in a potent antagonist in the [^{35}S]GTPγS binding assays at hA_3 ARs. In fact, while it does not affect the [^{35}S]GTPγS binding in the absence of NECA, it inhibits the NECA-stimulated [^{35}S]GTPγS binding with an EC_{50} value of 5.4 nM (Figure 1).

A structure−activity relationship (SAR) study of derivatives **1**−**6** and **13**−**16** provided some useful insights about the role of the electronic and steric properties of the 2-(*p*-phenyl) substituent on the two series **A** and **B** for hA_3 receptor−ligand recognition. The electronic properties of the 2-(*p*-phenyl) substituent do not seem to play a crucial role in the interaction of the 1,4-dione series derivatives with the receptor binding pocket. In fact, the most active compounds **1**, **1A**, and **6** bear either an electron-donating (OMe) or an electron-withdrawing (NO_2, OCOMe) substituent. More important roles seem to be exerted by the steric properties of the *p*-phenyl substituent and especially by its capability

Scheme 1[a]

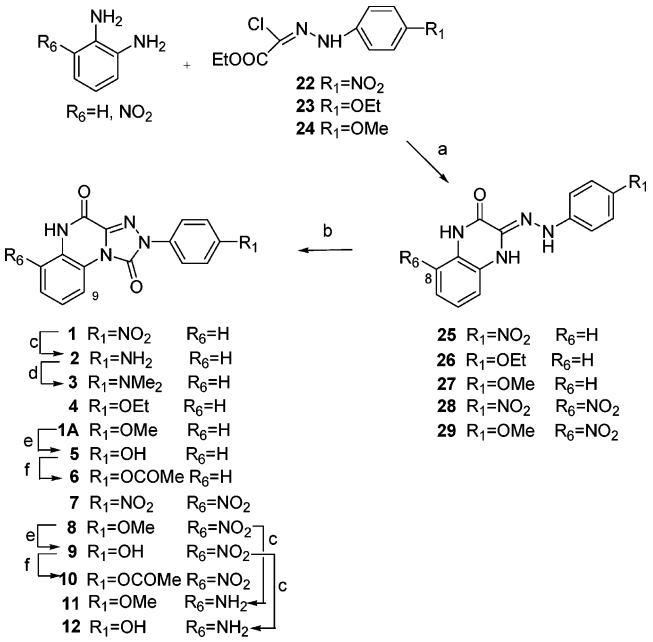

[a] (a) Et_3N, EtOH; (b) $(Cl_3CO)_2CO$, THF; (c) H_2, Pd/C, DMF; (d) 40% HCHO, $NaBH_3CN$, CH_3CN; (e) 48% HBr, AcOH; (f) Et_3N, $ClCOCH_3$, THF.

Scheme 2[a]

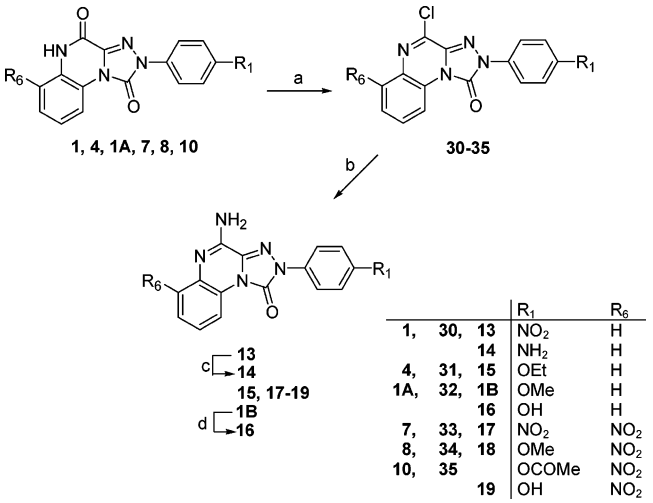

			R_1	R_6
1,	30,	13	NO_2	H
		14	NH_2	H
4,	31,	15	OEt	H
1A,	32,	1B	OMe	H
		16	OH	H
7,	33,	17	NO_2	NO_2
8,	34,	18	OMe	NO_2
10,	35		OCOMe	NO_2
		19	OH	NO_2

[a] (a) $PCl_5/POCl_3$, pyridine; (b) NH_3(g), absolute EtOH; (c) H_2, Pd/C, DMF; (d) 48% HBr, AcOH.

Scheme 3[a]

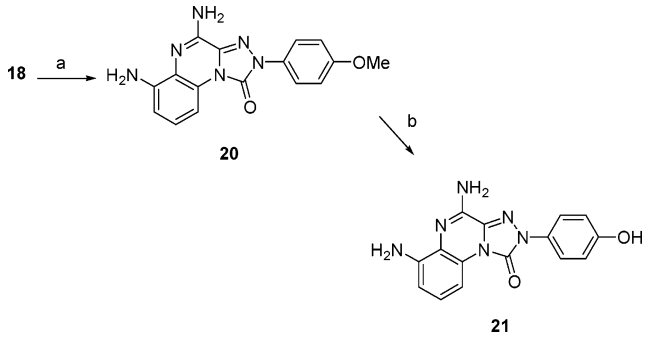

[a] (a) H_2, Pd/C, DMF; (b) BBr_3, CH_2Cl_2.

of acting as a hydrogen-bond acceptor. In fact, the subnanomolar A_3 AR affinity of compound **1**, significantly higher than those of the other compounds of series **A**, could suggest that the *p*-nitro substituent engages a hydrogen bond with a receptor proton donor site. This hypothesis is consistent with the binding affinities of compounds **1A** and **5** (R_1 = OH) and also explains the low A_3 binding affinity of derivative **2**, bearing the very weak hydrogen-bond acceptor *p*-amino group. When this substituent was replaced by the stronger hydrogen-bond acceptor *p*-dimethylamino group (compound **3**), an 8-fold enhancement of the A_3 affinity was obtained. The important role played by the steric bulk of the *p*-phenyl substituent is suggested by comparing the binding affinity of compound **1A** with that of the 10-fold less active 2-(4-ethoxyphenyl) derivative **4**. To test our hypothesis that both steric bulk and hydrogen-bonding interaction play a key role in the anchoring of the 2-aryl moiety of our triazoloquinoxaline derivatives to the hA_3 AR, we rationally synthesized the 2-(4-acetoxyphenyl) derivative **6**. In fact, the acetoxy group is similar to the ethoxy group from a steric point of view, but it is a stronger hydrogen-bond acceptor because of the carbonyl group oxygen. As we expected, compound **6** exhibits 16-fold higher hA_3 affinity compared to **4**.

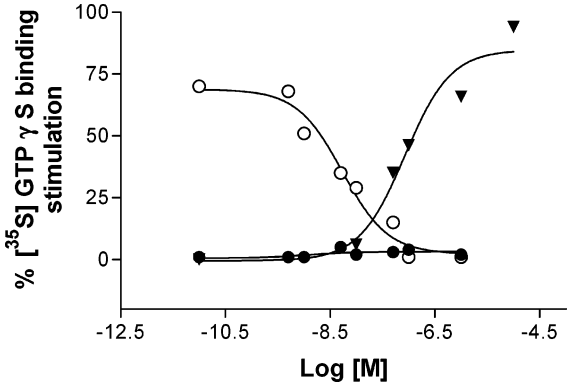

Figure 1. [^{35}S]GTPγS binding assays at hA_3 ARs: stimulation curve of [^{35}S]GTPγS binding by different concentrations of NECA (▼); modulation curve of [^{35}S]GTPγS binding by different concentrations of compound **1** in the absence of NECA (●); inhibition curve of NECA-stimulated (10 μM) [^{35}S]GTPγS binding by different concentrations of compound **1** (○). Curves are representative of single experiments performed three times with similar results. EC_{50} ± SEM values for NECA and compound **1** were 84.8 ± 9.2 and 5.4 ± 0.8 nM, respectively.

In series **B**, replacement of the *p*-methoxy substituent of the lead **1B** with other groups (compounds **13**−**16**) modulates the hA_3 affinity to a minor extent with respect to series **A**. Most of the *p*-phenyl-substituted derivatives (compounds **14**−**16**) possess good A_3 affinity even though none of them are more active than the lead compound **1B**. In particular, it is noted that the 2-(4-nitrophenyl) derivative **13**, in contrast to the corresponding 1,4-dione derivative **1**, is completely inactive at the A_3 subtype. The SARs of series **B** resemble those discussed above for series **A**. In series **B** the steric properties of the 2-(*p*-phenyl) substituent, as well as its capability of engaging a hydrogen bond, also play a role in hA_3 receptor recognition. In fact, derivative **16**, bearing a hydrogen-bond acceptor, i.e., the *p*-hydroxy group, is equiactive to **1B**, while the 2-(4-aminophenyl) derivative **14** shows a 7-fold lower hA_3 affinity than **1B**. The importance of steric bulk is shown by the about 5-fold lower hA_3 affinity of the 2-(4-ethoxyphenyl) derivative **15** with respect to **1B**.

In the second phase of the work we variously combined the R_1 substituents that were most advantageous for A_3 affinity and/or selectivity (R_1 = OMe, OH, OCOMe, NO_2) with the 6-nitro group (compounds **7**−**10** and **17**−**19**) to verify whether the positive effects of all these substituents were additive. The binding results show that in series **A** only the combination of the 6-nitro group with the 2-(4-methoxyphenyl) substituent positively affected both hA_3 affinity and selectivity. In fact, compound **8** exhibits high hA_3 affinity and higher hA_3 vs hA_1 selectivity than its lead compound **1A**, while compounds **7** ($R_1 = NO_2$), **9** (R_1 = OH), and **10** (R_1 = OCOMe) are completely devoid of A_3 affinity. A similar trend is observed in the double substituted derivatives **17**−**19** of series **B**. In fact, also in this series, only the combination of the 6-nitro group with the 2-(4-methoxyphenyl) substituent (compound **18**) affords nanomolar hA_3 affinity and higher hA_3 vs hA_1 selectivity, compared to the lead compounds **1B** and **2B**.[17] In contrast, the 6-nitro derivatives **17** ($R_1 = NO_2$) and **19** (R_1 = OH) are completely inactive at the hA_3 ARs. Finally, the 6-nitro derivatives **8**, **9**, **18**, and **19** were reduced to the corresponding 6-amino derivatives **11**, **12**, **20**, and **21** because in previous studies the presence of the 6-amino substituent on our triazoloquinoxaline derivatives was advantageous to hA_3 affinity.[17] In the present study, this transformation causes different effects in series **A** and **B**. In the former, the 6-amino compound **11** is 17-fold less active than the corresponding 6-nitro derivative **8** while the 6-amino compound **12** is totally inactive, similar to the 6-nitro derivative **9**. In contrast, in series **B**, the 6-amino compound **20** and **21** display, respectively, a 2-fold and a more than 6-fold enhanced A_3 affinity with respect to the corresponding 6-nitro derivatives **18** and **19**. Nevertheless, the 6-amino derivative **20** is less hA_3 vs hA_1 selective than **18**, showing only a 8.4-fold selectivity ratio.

The binding data of compounds **1**−**21** also provided new insights about the structural requirements of the bA_1 AR. The bA_1 receptor seems to tolerate hydrophilic groups well. In fact, the 2-(4-aminophenyl) derivative **2** exhibits the highest bA_1 affinity (K_i = 8.7 nM) among the herein reported antagonists. Moreover, either the 2-(4-hydroxyphenyl) derivative **5** or the 2-(4-acetoxyphenyl)-substitued compound **6** possesses high bA_1 affinity. The advantageous effect of the hydrophilic *p*-amino and *p*-hydroxy groups on the 2-phenyl ring also emerged among derivatives **13**−**16** of series **B**, compounds **14** and **16** being the most active at the bA_1 ARs. The bA_1 binding affinities seem to be also influenced by the steric bulk of the substituent on the 2-phenyl ring. The lower A_1 affinities of the *p*-(dimethylamino) derivative **3** and of the *p*-ethoxy-substituted compound **4**, compared to those of **2** ($R_1 = NH_2$) and **1A** (R_1 = OMe), respectively, could be attributed not only to the increased lipophilicity but also to the higher steric hindrance of the dimethylamino and ethoxy groups with respect to the amino and methoxy substituents. A similar consideration can be made, although to a lesser degree, about **15** with respect to the corresponding lead compound **1B**. The binding activity of compound **6** exemplifies the importance of a proper balance between the steric bulk and hydrophobicity of the substituent for bA_1 receptor−ligand interaction. In fact, compound **6**, which shows a significantly higher bA_1 affinity (384-fold) than **4**, bears a *p*-acetoxy substituent that possesses a steric bulk similar to that of the ethoxy group (compound **4**) but with an increased hydrophilicity.

As we expected on the basis of our previous studies,[17] introduction of the 6-nitro group on the 2-aryl derivatives **1A**, **5**, **6**, and **1B** dramatically decreased the bA_1 affinity (see compounds **8**, **9**, **10** and **18**). In contrast, the 6-nitro-substituted derivatives **7**, **17**, and **19** display good affinities for this AR.

Reduction of the 6-nitro group of the 2-(4-methoxyphenyl) derivatives **8** and **18** afforded derivatives **11** and **20**, which are still inactive on the bA_1 AR. In contrast, the 6-amino-2-(4-hydroxyphenyl) derivatives **12** and **21** show a significantly higher bA_1 affinity than the corresponding 6-nitro compounds **9** and **19**.

A comparison of the bA_1 affinity values of compounds **1A**, **1**, **5**, **6**, **8**, **1B**, **2B**, **18**, and **20** with those determined at the hA_1 receptor indicates that these two receptors possess different structural requirements due to well-known species differences.[23,27] In fact, all the tested compounds exhibit bA_1 affinities different from those determined for hA_1 ARs.

Building an Antagonist-Bound Model of hA_3 Adenosine Receptor. The SAR analysis, discussed above, does not allow us to establish whether derivatives of the two series **A** and **B** interact with the hA_3 AR recognition site with a similar or different binding mode. In fact, although some SAR similarities could suggest an analogous approach in the binding cavity, the noted differences and especially the opposite behavior of the *p*-nitro-substituted derivatives **1** and **13** allow us to suppose a different orientation of the 1,4-diones (series **A**) and the 4-amino-1-one (series **B**) derivatives inside the recognition site. To interpret our experimental results, we decided to theoretically depict the putative transmembrane (TM) binding motif of triazoloquinoxaline analogues on hA_3 AR. Following our recently reported modeling approach,[28−30] we built an improved model of the hA_3 receptor, using the bovine rhodopsin crystal structure as template,[31] which can be considered a further refinement in building the hypothetical binding site of the previously proposed A_3 AR antagonists. Special attention had to be given to the second extracellular (E2) loop, which has been described in bovine rhodopsin to fold back over TM helices and therefore limits the size of the active site.[31] As Jacobson and coauthors have already demonstrated, amino acids of this loop could be involved in direct interactions with the ligands.[32] Details of the building model are given in the Experimental Section. As previously reported, the recognition of classic hA_3 AR antagonists seems to occur in the upper region of the TM helical bundle. TMs 3, 5, 6, and 7 appear to be crucial for the recognition of both agonists and antagonists. Very recently, a number of amino acid residues in the TM domains 3 and 5 and the second extracellular loop (EL2) were individually replaced with Ala and other amino acids.[32] These residues are homologous to those predicted in previous molecular modeling studies of the adenosine receptor for ligand recognition, including His95, Trp243, Ser247, Asn250, and Lys152.

The first interesting result obtained from our molecular docking studies is that the 2-(*p*-nitrophenyl)-

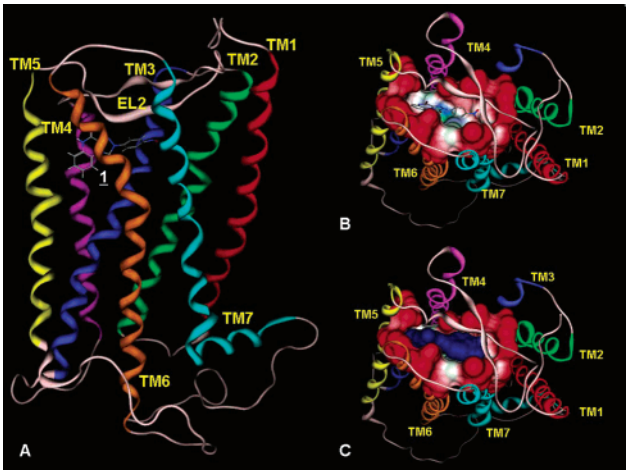

Figure 2. hA_3 receptor model viewed from the membrane side (A) and from the extracellular side (B) showing the E2 loop folded into the binding crevice. Putative binding sites, suggested by site-directed mutagenesis studies, is delimited by the docked derivative **1**. The steric complementarity between the ligand (derivative **1**) and the receptor cavity is shown in part C.

substituted derivative **1** can fit nicely inside the TM region of hA_3 AR. As shown in Figure 2, the binding of the triazoloquinoxaline moiety seems to occur in the upper region of the helical bundle. A very clear steric and electrostatic complementarity has been found between derivative **1** and the hypothetical binding cavity on hA_3 AR. At least six stabilizing hydrogen-bonding interactions have been described using the most energetically stable docked conformation (see Experimental Section for details). Thr94 (TM3), His95 (TM3), Trp243 (TM6), Asn250 (TM6), His272 (TM7), Ser165 (EL2), and Gln167 (EL2) seem to characterize the ligand recognition region on the receptor. Accordingly, the triazoloquinoxaline nucleus should be most favorably oriented perpendicular to the plane of the lipid bilayer, with the 2-aryl substituent in proximity to TM2 and TM7 and the fused benzene ring close to TM5 and TM6. Several important hydrophilic contacts, probably hydrogen-bonding interactions, seem to be involved among the two carbonyl groups of the triazoloquinoxaline moiety and some of the residues oriented inside the TM bundle, such as Thr94 (TM3), His95 (TM3), Asn250 (TM6), and Gln167 (EL2).

As previously underlined, the 2-(*p*-nitrophenyl) substituent on compound **1** is crucial for high potency and selectivity. As described above, the 2-aryl substituent is positioned in a small cleft defined by EL2, TM2, and TM7. This peculiar hydrophobic pocket is delimited by nonpolar amino acids such as Leu90 (TM3), Leu246 (TM6), and Ile268 (TM7). However, two extremely crucial polar residues, such as Ser165 (EL2) and His272 (TM7), are also present at the border of this hydrophobic pocket. In our model, the nitro group of derivative **1** is able to strongly achieve two hydrogen-bonding interactions with Ser165 and His272. These two hydrogen-bonding interactions seem to be responsible for the observed subnanomolar activity versus the hA_3 receptor. Accordingly, the replacement of the $-NO_2$ with other hydrogen-bond acceptors, as well as −OCOMe (**6**) and −OMe (**1A**), is still acceptable even if the interaction energies are less favorable. On the other hand, the replacement of the nitro with the amino hydrogen-bond donor (**2**) drastically reduces the hA_3 AR affinity. The presence of bulky and weak hydrogen-bond acceptors such as −OEt (**4**) or $-NMe_2$ (**3**) also produces a modest affinity to the hA_3 AR. The amphiphatic behavior of −OH as hydrogen-bond acceptor and donor reduces the affinity of derivative **5** without, in any case, abolishing it.

In general, the concurrent presence, on the triazoloquinoxaline-1,4-dione moiety, of the 6-nitro substituent and the 2-(*p*-phenyl) substituent is not well tolerated (compounds **7**, **9**, **10**). The fused benzene ring of the triazoloquinoxaline moiety is positioned into a tiny hydrophobic fissure originated by TM5 and TM6. The double substitution sensibly increases the volume of the antagonist structure neglecting its appropriate binding with the receptor cavity. Only the 6-NO_2 group and the 2-(*p*-methoxyphenyl) substituent together are still tolerated (compound **8**). In this case, the small methoxy group can still be positioned in the small hydrophobic fissure originated by TM2 and TM7. Accordingly, all docked double substituted triazoloquinoxaline derivatives have been characterized by high van der Waals repulsion energies during all of the molecular docking simulations.

From a classical structure−activity relationship point of view, as explained above, the comparison between derivatives **1** and **13**, both with the 2-(*p*-nitrophenyl) substitution, at first glance depicts an irrational scenario. Surprisingly, derivative **13** is almost inactive against the hA_3 receptor. On the other hand, derivative **2B** with a nitro group at the 6-position presents a high nanomolar activity versus the same receptor. Consequently, the replacement of the 4-carbonyl group of the triazoloquinoxaline moiety with an amino group drastically changed the structure−activity relationships already proposed. A convincing answer to this dilemma can be found from our molecular docking simulations. Inside the binding cavity, the orientations of the two triazoloquinoxaline moieties, the 2-aryl-1,2,4-triazolo[4,3-*a*]quinoxaline-1,4-diones (series **A**) and 2-aryl-1,2,4-triazolo[4,3-*a*]quinoxalin-4-amino-1-ones (series **B**), are surprisingly different. As shown in Figure 3, the replacement of the carbonyl group with the amino substituent flips the orientation of the triazoloquinoxaline moiety by 180° with respect to the original one. In this new situation, the triazoloquinoxaline nucleus is still favorably oriented perpendicular to the plane of the lipid bilayer but with the 2-aryl substituent in proximity to TM5 and TM6 and the fused benzene ring close to TM2 and TM7. The 2-(*p*-nitrophenyl) position of derivative **1** is almost in correspondence with the 6-position of derivative **2B**. This molecular flip inside the binding cavity seems to be aimed at preserving the hydrogen-bonding interactions among the triazoloquinoxaline moiety and the most crucial amino acids of the binding cavity. In particular, the 6-nitro group of derivative **2B** can still interact through two hydrogen bonds with Ser165 (EL2) and His272 (TM7). Moreover, further evidence supporting our hypothesis about the flipped conformation can be obtained from the analysis of docking results concerning the already published 2-phenyl-6-nitro-1,2,4-triazolo[4,3-*a*]quinoxaline-1,4-diones (namely, compound **7** in ref 17). This compound presents a

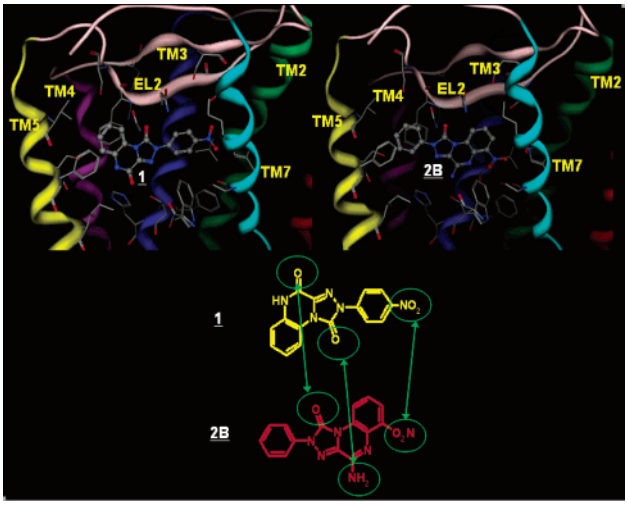

Figure 3. Triazoloquinoxaline derivatives binding site in the hA_3 receptor: derivatives **1** (upper-left side) and **2B** (upper-right side) docked into the ligand binding crevice of the human A_3 receptor viewed from the membrane side facing TM helices 5 and 6. H-bonding interactions are shown by the dashed line. Hydrogen atoms are not displayed.

high nanomolar range activity versus the hA_3 receptor (K_i = 279 nM).[17] This derivative shares the peculiar binding conformation of all series **A** compounds bearing the 6-nitro group positioned in the tiny hydrophobic fissure originated by TM5 and TM6, as already described for derivative **13**. The steric hindrance of the 6-nitro moiety with both TM5 and TM6 and the lost possibility of directly interacting with EL2 and His272 (TM7) drastically reduce the hA_3 AR binding affinity. As previously speculated for series **A**, also for series **B** the simultaneous presence on the triazoloquinoxaline moiety of the 6-nitro substituent and of the *p*-nitro or *p*-hydroxy groups on the 2- phenyl ring (compounds **17** and **19**, respectively) is not well tolerated.

Conclusion

The present study has highlighted that the 1,2,4-triazolo[4,3-*a*]quinoxalin-1-one moiety is an attractive scaffold for obtaining potent and selective hA_3 AR antagonists. The classical SAR analysis, supported by molecular modeling studies, provides new useful insights about the steric, lipophilic, and electrostatic requirements that are important for the optimal anchoring of these derivatives to the hA_3 AR recognition site. Advances in the general methods of molecular modeling and the resolution of the template structures of rhodopsin have brought this integrated perspective to a stage of practicality as a medicinal chemical approach to studying GPCRs in general and purine/pyrimidine receptors specifically. Ligand−receptor modeling studies have clarified the binding mode of our triazoloquinoxaline derivatives and have provided insights into the putative binding sites and recognition elements. Identification of microscopic complementarity between residues of the putative receptor binding site and the docked high-affinity ligands (i.e., energetically stabilizing elements in ligand recognition) has aided in the design process. The ligand−receptor modeling studies have pointed out that (i) several hydrogen-bonding interactions seem to be crucial for the anchoring of this class of antagonists to the hA_3 AR recognition site, (ii) both the 2-aryl group and the fused benzene ring interact with two size-limited binding pockets and, as a consequence, the volume of the whole molecule is critical in the fitting with the receptor, and (iii) the orientations of the 1,4-dione (series **A**) and 4-amino-1-one derivatives (series **B**) inside the binding site are probably different. Taking into account these new findings, further modifications of these compounds to improve A_3 AR affinity and selectivity are in progress.

Experimental Section

(A) Chemistry. Silica gel plates (Merck F_{254}) and silica gel 60 (Merck, 70−230 mesh) were used for analytical and column chromatography, respectively. All melting points were determined on a Gallenkamp melting point apparatus. Microanalyses were performed with a Perkin-Elmer 260 elemental analyzer for C, H, N, and the results were within ±0.4% of the theoretical unless otherwise stated. The IR spectra were recorded with a Perkin-Elmer Spectrum RX I spectrometer in Nujol mulls and are expressed in cm^{-1}. The ^1H NMR spectra were obtained with a Varian Gemini 200 instrument at 200 MHz. The chemical shifts are reported in δ (ppm) and are relative to the central peak of the solvent that is always DMSO-d_6.

General Procedure for the Synthesis of 1,2,3,4-Tetrahydro-3-arylhydrazonoquinoxalin-2-ones 25,[18] 26, 27,[16,18] 28, 29. Compounds **26**, **28**, and **29** were obtained following the reported procedure[16,18] described to prepare compounds **25** and **27**. Briefly, ethyl N^1-arylhydrazono-N^2-chloroacetates **22**−**24**[19−21] (9 mmol) were reacted with 1,2-phenylenediamine (9 mmol) in refluxing ethanol (80 mL) and triethylamine (10.8 mmol) for 3 h. The suspension was cooled at room temperature, and the solid, made up of **25**−**27**, was collected by filtration and washed with water (30−40 mL). Similarly, when **22** and **24** reacted with the 3-nitro-1,2-phenylenediamine, compounds **28** and **29** were obtained, respectively. Compounds **26**, **28**, **29**, as previously described for **25**[18] and **27**,[16,18] may exist in either tautomeric forms **a** and **b**:

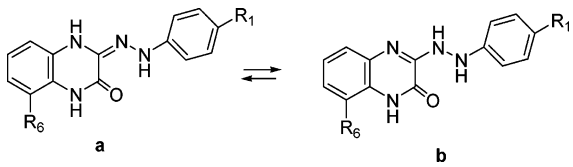

In fact, their ^1H NMR spectra revealed the existence of both tautomers because there are more than three signals relative to protons that exchange with D_2O.

26: yield 90%; mp 226−228 °C dec (EtOH); ^1H NMR δ 1.08−1.38 (m, CH_3 of both tautomers), 3.83−3.94 (m, CH_2 of both tautomers), 6.65−7.29 (m, ar), 8.49 (br s, NH), 9.36 (br s, NH), 9.47 (br s, NH), 11.09 (br s, NH), 12.29 (br s, NH). Anal. ($C_{16}H_{16}N_4O_2$) C, H, N.

28: yield 85%; mp 283−285 °C dec (DMF); ^1H NMR δ 6.80−7.08 (m, ar), 7.98−8.19 (m, ar + NH), 8.21−8.27 (m, ar,), 9.28 (br s, NH), 10.22 (br s, NH), 12.08 (br s, NH). Anal. ($C_{14}H_{10}N_6O_5$) C, H, N.

29: yield 80%; mp 155−157 °C dec (AcOH); ^1H NMR δ 3.68 (s, OCH_3), 6.68−7.40 (m, ar), 7.62−7.70 (m, ar + NH), 7.92−7.98 (m, ar), 8.84 (br s, NH), 9.89 (br s, NH), 9.97 (br s, NH), 10.31 (br s, NH), 11.40 (br s, NH). Anal. ($C_{15}H_{13}N_5O_4$) C, H, N.

General Procedure for the Synthesis of 1,2,4,5-Tetrahydro-2-aryl-1,2,4-triazolo[4,3-*a*]quinoxaline-1,4-diones 1,[18] 4, 1A,[16,18] 7, 8. Compounds **4**, **7**, and **8** were prepared by reacting compounds **26**, **28**, and **29** (4 mmol), respectively, with triphosgene (4 mmol) in refluxing anhydrous tetrahydrofuran (40 mL) for 2−3 h, as described to prepare **1**[18] and **1A**[16,18] from **25** and **27**, respectively.

4: yield 95%; mp >300 °C (AcOH); ^1H NMR δ 1.35 (t, 3H, CH_3), 4.07 (q, 2H, CH_2), 7.09 (d, 2H, ar, J = 9.2 Hz), 7.26−

7.35 (m, 3H, ar), 7.85 (d, 2H, ar, J = 9.2 Hz), 8.59 (d, 1H, H-9, J = 8.1 Hz), 11.94 (s, 1H, NH). Anal. ($C_{17}H_{14}N_4O_3$) C, H, N.

7: yield 89%; mp >300 °C (DMF); ^{1}H NMR δ 7.53 (t, 1H, ar, J = 8.1 Hz), 8.13 (d, 1H, ar, J = 7.0 Hz), 8.31 (d, 2H, ar, J = 9.5 Hz), 8.45 (d, 2H, ar, J = 9.5 Hz), 8.99 (d, 1H, H-9, J = 6.9 Hz), 11.38 (br s, 1H, NH); IR 1707, 3324. Anal. ($C_{15}H_8N_6O_6$) C, H, N.

8: yield 85%; mp 262−264 °C (AcOH); ^{1}H NMR δ 3.80 (s, 3H, CH_3), 7.12 (d, 2H, ar, J = 9.16 Hz), 7.49 (t, 1H, H-8, J = 8.3 Hz), 7.85 (d, 2H, ar, J = 9.1 Hz), 8.12 (d, 1H, H-7, J = 8.3 Hz), 9.02 (d, 1H, H-9, J = 8.1 Hz), 11.25 (s, 1H, NH). Anal. ($C_{16}H_{11}N_5O_5$) C, H, N.

2-(4-Aminophenyl)-1,2,4,5-tetrahydro-1,2,4-triazolo-[4,3-*a*]quinoxaline-1,4-dione (2).[18] The title compound was prepared from **1** as described in ref 18.

2-(4-Dimethylaminophenyl)-1,2,4,5-tetrahydro-1,2,4-triazolo[4,3-*a*]quinoxaline-1,4-dione (3). Aqueous formaldehyde (40%, 0.74 mL) was added to a suspension of **2** (0.85 mmol) in acetonitrile (15 mL). The mixture was stirred at room temperature for 5 min, then sodium cyanoborohydride (2.9 mmol) was added. After the mixture was stirred for 6 h at room temperature, a second portion of aqueous formaldehyde (40%, 0.74 mL) and sodium cyanoborohydride (2.9 mmol) was added and the suspension was left overnight at room temperature. After dilution with water (10 mL), the mixture was acidified with glacial acetic acid and the solid was collected and washed with water. Yield: 95%; mp >300 °C (DMF/EtOH); ^{1}H NMR δ 2.94 (s, 6H, 2CH_3), 6.85 (d, 2H, ar, J = 9.1 Hz), 7.21−7.40 (m, 3H, ar), 7.71 (d, 2H, ar, J = 9.1 Hz), 8.60 (d, 1H, H-9, J = 8.1 Hz), 11.90 (s, 1H, NH); IR 1690, 1730, 3160 cm^{-1}. Anal. ($C_{17}H_{15}N_5O_2$) C, H, N.

2-(4-Hydroxyphenyl)-1,2,4,5-tetrahydro-1,2,4-triazolo-[4,3-*a*]quinoxaline-1,4-dione (5).[18] The title compound was obtained from **1A** as described in ref 18.

2-(4-Acetoxyphenyl)-1,2,4,5-tetrahydro-1,2,4-triazolo-[4,3-*a*]quinoxaline-1,4-dione (6). A mixture of compound **5**[18] (0.68 mmol), triethylamine (2.72 mmol), and acetyl chloride (0.68 mmol) in anhydrous tetrahydrofuran (20 mL) was refluxed for 3 h. After the mixture was cooled at room temperature, the solid was filtered off and the solvent of the clear solution was evaporated at reduced pressure. The residue was purified on silica gel column, eluting with chloroform/methanol (11:0.5). Evaporation of the solvent of the second eluates afforded compound **6**. Yield: 62%; mp 298−299 °C (DMF); ^{1}H NMR δ 2.30 (s, 3H, CH_3), 7.22−7.41 (m, 5H, ar), 8.02 (d, 2H, ar, J = 9.2 Hz), 8.60 (d, 1H, H-9, J = 8.1 Hz), 11.99 (s, 1H, NH); IR 1690, 1720, 1770, 3390 cm^{-1}. Anal. ($C_{17}H_{12}N_4O_4$) C, H, N.

2-(4-Hydroxyphenyl)-6-nitro-1,2,4,5-tetrahydro-1,2,4-triazolo[4,3-*a*]quinoxaline-1,4-dione (9). A suspension of compound **8** (1.4 mmol) in glacial acetic acid (2 mL) and hydrobromic acid (48%, 9 mL) was refluxed for 40 h. After the mixture was cooled at room temperature, the solid was filtered and washed with water. Yield: 86%; mp >300 °C (DMF); ^{1}H NMR δ 6.91 (d, 2H, ar, J = 8.8 Hz), 7.47 (t, 1H, ar, J = 8.4 Hz), 7.71 (d, 2H, ar, J = 8.8 Hz), 8.10 (d, 1H, ar, J = 8.4 Hz), 9.01 (d, 1H, H-9, J = 8.4 Hz), 9.82 (s, 1H, OH), 11.22 (s, 1H, NH); Anal. ($C_{15}H_9N_5O_5$) C, H, N.

2-(4-Acetoxyphenyl)-6-nitro-1,2,4,5-tetrahydro-1,2,4-triazolo[4,3-*a*]quinoxaline-1,4-dione (10). A mixture of compound **9** (0.58 mmol), acetyl chloride (0.87 mmol), and triethylamine (0.87 mmol) in anhydrous tetrahydrofuran (20 mL) was refluxed for 12 h. The suspension was cooled at room temperature, and the solid was collected by filtration and washed with water. Yield: 90%; mp 266−268 °C (DMF); ^{1}H NMR δ 2.29 (s, 3H, CH_3), 7.34 (d, 2H, ar, J = 9.1 Hz), 7.50 (t, 1H, ar, J = 8.4 Hz), 8.01 (d, 2H, ar, J = 8.8 Hz), 8.14 (d, 1H, ar, J = 8.1 Hz), 9.01 (d, 1H, H-9, J = 8.1 Hz), 11.30 (s, 1H, NH). Anal. ($C_{17}H_{11}N_5O_6$) C, H, N.

6-Amino-2-(4-methoxyphenyl)-1,2,4,5-tetrahydro-1,2,4-triazolo[4,3-*a*]quinoxaline-1,4-dione (11). A mixture of compound **8** (0.79 mmol) and 10% Pd/C (30 mg) in hot ethyl acetate (200 mL) was hydrogenated in a Parr apparatus at 30 psi for 1 h. After evaporation of the solvent at reduced pressure, the residue was suspended in hot DMF (8 mL) and the catalyst was filtered off. The solution was diluted with water, and the solid was collected by filtration. Yield: 50%; mp >300 °C (AcOH); ^{1}H NMR δ 3.79 (s, 3H, CH_3), 5.60 (s, 2H, NH_2), 6.68 (t, 1H, ar, J = 8.4 Hz), 6.98 (t, 1H, ar, J = 8.4 Hz), 7.09 (d, 2H, ar, J = 8.8 Hz), 7.84 (d, 2H, ar, J = 8.8 Hz), 7.93 (d, 1H, ar, J = 8.4 Hz), 10.98 (s, 1H, NH). Anal. ($C_{16}H_{13}N_5O_3$) C, H, N.

6-Amino-2-(4-hydroxyphenyl)-1,2,4,5-tetrahydro-1,2,4-triazolo[4,3-*a*]quinoxaline-1,4-dione (12). A mixture of the 6-nitro derivative **9** (1.03 mmol) and 10% Pd/C (0.03 g) in dimethylformamide (30 mL) was hydrogenated in a Parr apparatus at 30 psi for 12 h. The catalyst was filtered off, and the clear solution diluted with water gave a solid that was collected by filtration and washed with water and ethanol. Yield 94%; mp >300 °C (EtOH/DMF); ^{1}H NMR δ 5.62 (s, 2H, NH_2), 6.70 (d, 1H, ar, J = 7.3 Hz), 6.85−7.05 (m, 3H, ar), 7.72 (d, 2H, ar, J = 8.9 Hz), 7.95 (d, 1H, ar, J = 7.3 Hz), 9.56 (s, 1H, OH), 10.99 (s, 1H, NH). Anal. ($C_{15}H_{11}N_5O_3$) C, H, N.

General Procedure for the Synthesis of 2-Aryl-4-chloro-1,2-dihydro-1,2,4-triazolo[4,3-*a*]quinoxalin-1-ones 30, 31, 32,[16] 33−35. Compounds **30**, **31**, **33**, **34**, and **35** were obtained from **1**, **4**, **7**, **8** and **10**, respectively, following the reported procedure[16] to obtain **32** from **1A**. Briefly, a mixture of **1**,[16,18] **4**, **7**, **8**, and **10** (2 mmol), phosphorus pentachloride (4 mmol) in phosphorus oxychloride (40 mL), and anhydrous pyridine (0.2 mL) was refluxed until the disappearance (TLC monitoring) of the starting material (12−24 h). Evaporation of the excess phosphorus oxychloride at reduced pressure gave a residue that was treated with iced water (50 mL), collected, and washed with water and then cyclohexane. The 4-chloro derivatives **30**, **31**, **33**−**35**, obtained in high overall yields (80−90%), were unstable upon recrystallization; however, they were pure enough to be used without purification.

30: ^{1}H NMR δ 7.58−7.65 (m, 1H, ar), 7.78 (t, 1H, ar, J = 8.8 Hz), 7.91 (d, 1H, ar, J = 8.8 Hz), 8.35 (d, 2H, ar, J = 9.2 Hz), 8.47 (d, 2H, ar, J = 9.2 Hz), 8.72 (d, 1H, H-9, J = 7.3 Hz).

31: ^{1}H NMR δ 1.33 (t, 3H, CH_3, J = 8.6 Hz), 4.05 (q, 2H, CH_2, J = 8.6 Hz), 7.08 (d, 2H, ar, J = 8.8 Hz), 7.22−8.05 (m, 5H, ar), 8.71 (d, 1H, H-9, J = 8.1 Hz).

33: ^{1}H NMR δ 7.95 (t, 1H, H-8, J = 8.4 Hz), 8.09 (d, 1H, H-7, J = 8.4 Hz), 8.32−8.50 (m, 4H, ar), 8.91 (d, 1H, H-9, J = 6.7 Hz).

34: ^{1}H NMR δ 3.81 (s, 3H, OCH_3), 7.13 (d, 2H, ar, J = 9.1 Hz), 7.87−7.98 (m, 3H, ar), 8.05 (d, 1H, ar, J = 6.6 Hz), 8.94 (d, 1H, ar, J = 8.1 Hz).

35: ^{1}H NMR δ 2.31 (s, 3H, $COCH_3$), 7.37 (d, 2H, ar, J = 8.8 Hz), 7.90−8.12 (m, 4H, ar), 8.93 (d, 1H, H-9, J = 8.1 Hz).

General Procedure for the Synthesis of 4-Amino-2-aryl-1,2-dihydro-1,2,4-triazolo[4,3-*a*]quinoxalin-1-ones 13, 15, 17−19, 1B.[16] Compounds **13**, **15**, and **17**−**19** were prepared as previously described to obtain **1B** from **32**,[16] i.e., by heating overnight at 120 °C in a sealed tube a suspension of **30**, **31**, and **33**−**35** (2 mmol) in absolute ethanol (30 mL) saturated with ammonia. After the mixture was cooled, the solid was collected and washed with water.

13: yield 80%; mp >300 °C (DMF); ^{1}H NMR δ 7.30−7.45 (m, 3H, ar), 7.61 (br s, 2H, NH_2), 8.37 (d, 2H, ar, J = 8.8 Hz), 8.47 (d, 2H, ar, J = 8.8 Hz), 8.57 (d, 1H, H-9, J = 6.7 Hz); IR 1713, 3434 cm^{-1}. Anal. ($C_{15}H_{10}N_6O_3$) C, H, N.

15: yield 82%; mp 246−248 °C (2-ethoxyethanol); ^{1}H NMR δ 1.35 (t, 3H, CH_3, J = 7.0 Hz), 4.04 (q, 2H, CH_2, J = 7.0 Hz), 7.08 (d, 2H, ar, J = 9.1 Hz), 7.21−7.47 (m, 5H, 3 ar + NH_2), 7.88 (d, 2H, ar, J = 9.1 Hz), 8.60 (d, 1H, H-9, J = 7.7 Hz); IR 1718, 3299, 3461 cm^{-1}. Anal. ($C_{17}H_{15}N_5O_2$) C, H, N.

17: yield 70%; mp >300 °C (DMF); ^{1}H NMR δ 7.38 (t, 1H, ar, J = 8.1 Hz), 7.75 (d, 1H, ar, J = 8.1 Hz), 8.21 (br s, 2H, NH_2), 8.36 (d, 2H, ar, J = 9.1 Hz), 8.48 (d, 2H, ar, J = 9.1 Hz), 8.73 (d, 1H, H-9, J = 8.4 Hz); IR 1728, 3361, 3469 cm^{-1}. Anal. ($C_{15}H_9N_7O_5$) C, H, N.

18: yield 85%; mp 289−291°C (AcOH/DMF); ^{1}H NMR δ 3.80 (s, 3H, CH_3), 7.11 (d, 2H, ar, J = 9.1 Hz), 7.34 (t, 1H, ar, J = 8.4 Hz), 7.71 (d, 1H, ar, J = 7.7 Hz), 7.89 (d, 2H, ar, J = 9.1

Hz), 8.06 (br s, 2H, NH_2), 8.75 (d, 1H, H-9, J = 8.1 Hz). Anal. ($C_{16}H_{12}N_6O_4$) C, H, N.

19: yield 76%; mp >300 °C (2-methoxyethanol); ^{1}H NMR δ 6.90 (d, 2H, ar, J = 8.8 Hz), 7.35 (t, 1H, ar, J = 8.1 Hz), 7.62−8.01 (m, 3H, ar), 8.08 (br s, 2H, NH_2), 8.75 (d, 1H, ar, J = 8.4 Hz), 9.77 (s, 1H, OH). Anal. ($C_{15}H_{10}N_6O_4$) C, H, N.

4-Amino-2-(4-aminophenyl)-1,2-dihydro-1,2,4-triazolo-[4,3-*a*]quinoxalin-1-one (14). Compound **13** (0.9 mmol) was dissolved in hot dimethylformamide (30 mL), and 10% Pd/C (0.10 g) was added. The mixture was hydrogented in a Parr apparatus at 30 psi for 3 h. The catalyst was filtered off and the solution was diluted with water to give a solid that was collected by filtration and washed with water and ethanol. Yield 58%; mp > 300 °C (2-methoxyethanol); ^{1}H NMR δ 5.34 (s, 2H, NH_2), 6.66 (d, 2H, ar, J = 8.4 Hz), 7.20−7.44 (m, 5H, 3ar + NH_2), 7. 54 (d, 2H, ar, J = 8.4 Hz), 8.61 (d, 1H, H-9, J = 8.2 Hz); IR 1720, 3304, 3402, 3460 cm^{-1}. Anal. ($C_{15}H_{12}N_6O$) C, H, N.

4-Amino-1,2-dihydro-2-(4-hydroxyphenyl)-1,2,4-triazolo-[4,3-*a*]quinoxalin-1-one (16). A suspension of **1B**[16] (0.97 mmol) in glacial acetic acid (2 mL) and hydrobromic acid (48%, 9 mL) was refluxed for 4 h. After the mixture was cooled at room temperature, the solid was collected and washed with water. Yield 95%; mp >300 °C (2-ethoxyethanol); ^{1}H NMR δ 6.89 (d, 2H, ar, J = 8.8 Hz), 7.21−7.46 (m, 5H, 3ar + NH_2), 7.75 (d, 2H, ar, J = 8.8 Hz), 8.60 (d, 1H, H-9, J = 7.7 Hz), 9.74 (br s, 1H, OH); IR 1690, 3200−3450 cm^{-1}. Anal. ($C_{15}H_{11}N_5O_2$) C, H, N.

4,6-Diamino-1,2-dihydro-2-(4-methoxyphenyl)-1,2,4-triazolo[4,3-*a*]quinoxalin-1-one (20). The title compound was obtained by catalytic reduction of **18**, following the experimental procedure described above to prepare **14**. Yield 64%; mp 261−263 °C (DMF); ^{1}H NMR δ 3.79 (s, 3H, CH_3), 5.33 (s, 2H, NH_2 at the 6-position), 6.65 (d, 1H, ar, J = 8.1 Hz), 6.97 (t, 1H, ar, J = 8.1 Hz), 7.09 (d, 2H, ar, J = 8.7 Hz), 7.23 (br s, 2H, NH_2 at the 4-position), 7.83−7.99 (m, 3H, ar); IR 1718, 3300, 3466 cm^{-1}. Anal. ($C_{16}H_{14}N_6O_2$) C, H, N.

4,6-Diamino-1,2-dihydro-2-(4-hydroxyphenyl)-1,2,4-triazolo[4,3-*a*]quinoxalin-1-one (21). A solution of boron tribromide in dichloromethane (1 M, 6.9 mL) was added dropwise at 0 °C, under nitrogen, to a stirred suspension of compound **20** (3.4 mmol) in anhydrous dichloromethane (10 mL). The reaction mixture was allowed to proceed at 0 °C for 2 h and then at room temperature for 24 h. The mixture was then diluted with water and neutralized with 1 M NaOH solution. The solid was collected by filtration and washed with water. Yield 90%; mp 294−296 °C (EtOH); ^{1}H NMR δ 5.33 (br s, 2H, NH_2 at the 6-position), 6.65 (d, 1H, ar, J = 7.7 Hz), 6.80−7.01 (m, 3H, ar), 7.19 (br s, 2H, NH_2 at the 4-position), 7.74 (d, 2H, ar, J = 8.4 Hz), 7.85 (d, 1H, ar, J = 8.1 Hz), 9.71 (br s 1H, OH); IR 1703, 3183, 3318, 3390, 3462, 3513 cm^{-1}. Anal. ($C_{15}H_{12}N_6O_2$) C, H, N.

(B) Biochemistry. Bovine A_1 and A_{2A} Receptor Binding. Displacement of [^{3}H]CHA from A_1 ARs in bovine cerebral cortical membranes and [^{3}H]CGS 21680 from A_{2A} ARs in bovine striatal membranes was performed as described in ref 33.

Human A_1, A_{2A}, and A_3 Receptor Binding. Binding experiments at hA_1 and hA_3 ARs stably expressed in CHO cells were performed as previously described[17] using [^{3}H]CHA and [^{125}I]AB-MECA, respectively, as radioligands. Displacement of [^{3}H]NECA from hA_{2A} ARs stably expressed in CHO cells was performed as reported in ref 27.

The concentration of the tested compounds that produced 50% inhibition of specific [^{3}H]CHA, [^{3}H]CGS 21680, or [^{125}I]-AB-MECA binding (IC_{50}) was calculated using a nonlinear regression method implemented in the InPlot program (GraphPad, San Diego, CA) with five concentrations of displacer, each performed in triplicate. Inhibition constants (K_i) were calculated according to the Cheng−Prusoff equation.[34] The dissociation constant (K_d) of [^{3}H]CHA and [^{3}H]CGS 21680 in cortical and striatal bovine brain membranes were 1.2 and 14 nM, respectively. The K_d value of [^{3}H]CHA, [^{3}H]NECA, and [^{125}I]AB-MECA in hA_1, hA_{2A}, and hA_3 ARs in CHO cell membranes were 1.9, 30, and 1.4 nM, respectively.

[^{35}S]GTPγS Binding Assay. The [^{35}S]GTPγ S binding was carried out using CHO cells expressing hA_3 receptors. Membranes, prepared as previously described,[35] were suspended in a buffer containing 50 mM Tris, 3 U/mL adenosine deaminase, 100 mM NaCl, and 10 mM $MgCl_2$, pH 7.4, at a protein concentration of 10−20 μg per tube. The membrane suspension was preincubated in a final volume of 500 μL of buffer at 25 °C for 15 min with 1 μM GDP and different concentrations of the agonist NECA (10 nM to 10μM) or compound **1** (0.5 nM to 1 μM) alone or in the presence of 10 μM NECA. [^{35}S]GTPγ S (0.1 nM) was added, and the mixture was incubated for 60 min at 25 °C. The effect on nonspecific binding was determined in the presence of 10 μM GTPγS. Incubation was terminated by filtration over a GF/C glass fiber filter, and the sample was washed three times with the same buffer.

The EC_{50} values were calculated using the InPlot program with six to eight concentrations of ligand, each performed in triplicate.

(C) Computational Methodologies. All molecular modeling studies were carried out on a six-CPU (PIV 2.0−3.0 GHz) Linux cluster running under openMosix architecture.[36] Homology modeling, energy calculation, and docking studies were carried out using the Molecular Operating Environment (MOE, version 2003.03) suite.[37] The ground-state geometry of all charged and uncharged docked structures were fully optimized without geometry constraints using RHF/3-21G(*) ab initio calculations. Vibrational frequency analysis was used to characterize the minimum stationary points (zero imaginary frequencies). The software package Spartan O2 was utilized for all quantum mechanical calculations.[38]

Homology Model of the hA_3 AR. On the basis of the assumption that GPCRs share similar TM boundaries and overall topology,[31] a homology model of the hA_3 receptor was constructed. First, the amino acid sequences of TM helices of the A_3 receptor were aligned with those of bovine rhodopsin, guided by the highly conserved amino acid residues, including the DRY motif (D3.49, R3.50, and Y3.51) and three Pro residues (P4.60, P6.50, and P7.50) in the TM segments of GPCRs. The same boundaries were applied to the TM helices of the A_3 receptor, as identified from the X-ray crystal structure for the corresponding sequences of bovine rhodopsin, the C_α coordinates of which were used to construct the seven TM helices for the human A_3 receptor. The loop domains of the hA_3 receptor were constructed by the loop search method implemented in MOE. In particular, loops are modeled first in random order. For each loop, a contact energy function analyzes the list of candidates collected in the segment searching stage, taking into account all atoms already modeled and any atoms specified by the user as belonging to the model environment. These energies are then used to make a Boltzmann weighted choice from the candidates, the coordinates of which are then copied to the model. Any missing side chain atoms are modeled using the same procedure. Side chains belonging to residues whose backbone coordinates were copied from a template are modeled first, followed by side chains of modeled loops. Outgaps and their side chains were modeled last. Special caution had to be given to the second extracellular (E2) loop, which has been described in bovine rhodopsin to fold back over transmembrane helices[31] and therefore limits the size of the active site. Hence, amino acids of this loop could be involved in direct interactions with the ligands. A driving force to this peculiar fold of the E2 loop might be the presence of a disulfide bridge between cysteines in TM3 and E2. Since this covalent link is conserved in all receptors modeled in the current study, the E2 loop was modeled using a rhodopsin-like constrained geometry around the E2−TM3 disulfide bridge. After the heavy atoms were modeled, all hydrogen atoms were added, and the protein coordinates were then minimized with MOE using the AMBER94 force field.[39] The minimizations were carried out with 1000 steps of steepest descent followed by a conjugate gradient minimization until

the rms gradient of the potential energy was less than 0.1 kcal mol^{-1} $Å^{-1}$.

Molecular Docking of the hA_3 AR Antagonists. All antagonist structures were docked into the hypothetical TM binding site by using the DOCK docking program, part of the MOE suite. Searching is conducted within a user-specified 3D docking box, using the Tabù Search protocol[40] and the MMFF94 force field.[41−47] MOE-Dock performs a user-specified number of independent docking runs (50 in our specific case) and writes the resulting conformations and their energies to a molecular database file. The resulting docked complexes were subjected to MMFF94 energy minimization until the rms of the conjugate gradient was <0.1 kcal mol^{-1} $Å^{-1}$. Charges for the ligands were imported from the Spartan output files.

The interaction energy values were calculated as follows: $\Delta E_{binding} = E_{complex} - (E_{ligand} + E_{receptor})$. These energies are not rigorous thermodynamic quantities but can only be used to compare the relative stabilities of the complexes. Consequently, these interaction energy values cannot be used to calculate binding affinities because changes in entropy and solvation effects are not taken into account.

Acknowledgment. We thank Dr. Karl-Norbert Klotz of the University of Wüzburg, Germany, for providing cloned hA_1, hA_{2A} and hA_3 receptors expressed in CHO cells. We also thank Mr. Andrea Tralli for his involvement in the present molecular modeling study. S. Moro is very grateful to Chemical Computing Group for the scientific and technical collaboration.

Supporting Information Available: Analytical data for the compounds. This material is available free of charge via the Internet at http://pubs.acs.org.

References

(1) Fredholm, B. B.; Ijzerman, A. P.; Jacobson, K. A.; Klotz, K. N.; Linden, J. International union of pharmacology XXV. Nomenclature and classification of adenosine receptors. *Pharmacol. Rev.* **2001**, *53*, 527−552.

(2) Jacobson, K. A.; Knutsen, L. J. S. P1 and P2 purine and pyrimidine receptor ligands. In: *Purinergic and Pyrimidinergic Signalling*; Abbracchio, M. P., Williams, M., Eds.; Handbook of Experimental Pharmacology, Vol. 151/1; Springer: Berlin, 2001; pp 129−175.

(3) Linden, J.; Taylor, H. E.; Robeva, A. S.; Tucker, A. L.; Stehle, J. H.; Rivkees, S. A.; Fink, J. S.; Reppert, S. M. Molecular-cloning and functional expression of sheep A_3 adenosine receptor with widespread tissue distribution. *Mol. Pharmacol.* **1993**, *44*, 524−532.

(4) Gao, Z.-G.; Blaustein, J. B.; Gross, A. S.; Melman, N.; Jacobson, K. A. N6-Substituted adenosine derivatives: selectivity, efficacy and species differences at A_3 adenosine receptors. *Biochem. Pharmacol.* **2003**, *65*, 1675−1684.

(5) Jacobson, K. A.; Suzuki, F. Recent developments in selective agonists and antagonists acting at purine and pyrimidine receptors. *Drug. Dev. Res.* **1996**, *39*, 289−300.

(6) Abbracchio, M. P.; Brambilla, R.; Kim, H. O.; von Lubitz, D. K. J. E.; Jacobson, K. A.; Cattabeni, F. G-protein-dependent activation of phospholipase-C by adenosine A_3 receptor in rat brain. *Mol. Pharmacol.* **1995**, *48*, 1083−1045.

(7) Ali, H.; Choi, O. H.; Fraundorfer, P. F.; Yamada, K.; Gonzaga, H. M. S.; Beaven, M. A. Sustained activation of phospholipase-D via adenosine A_3 receptors is associated with enhancement of antigen-ionophore-induced and Ca^{2+}-ionophore-induced secretion in a rat mast-cell line. *J. Pharmacol. Exp. Ther.* **1996**, *276*, 837−845.

(8) (a) van Schaick, E. A.; Jacobson, K. A.; Kim, H. O.; Ijzerman, A. P.; Danhof, M. Haemodinamic effects and histamine release elicited by the selective adenosine A_3 receptor agonist 2-Cl-IB-MECA in conscious rats. *Eur. J. Pharmacol.* **1996**, *308*, 311−314. (b) Meade, C. J.; Mierau, J.; Leon, I.; Ensinger, H. A. In vivo role of the adenosine A_3 receptor: N6-2-(4-aminophenyl)-ethyladenosine induces broncospasm in BDE rats by a neurally mediated mechanism involving cells resembling mast cells. *J. Pharmacol. Exp. Ther.* **1996**, *279*, 1148−1156.

(9) (a) Forsythe, P.; Ennis, M. Adenosine, mast cells and asthma. *Inflammation Res.* **1999**, *48*, 301−307. (b) Marx, D.; Ezeamuzie, C. I.; Nieber, K.; Szelenyi, I. Therapy of bronchial asthma with adenosine receptor agonists or antagonists. *Drug News Perspect.* **2001**, *14*, 89−100.

(10) Brambilla, R.; Cattabeni, F.; Ceruti, S.; Barbieri, D.; Franceschi, C.; Kim, Y.-C.; Jacobson, K. A.; Klotz, K.-N.; Lohse, M. J.; Abbracchio, M. P.; Activation of the A_3 adenosine receptor affects cell cycle progression and cell growth. *Naunyn-Schmiedeberg's Arch. Pharmacol.* **2000**, *361*, 225−234.

(11) von Lubitz, D. K. J. E.; Lin, R. C. S.; Popik, P.; Carter, M. F.; Jacobson, K. A. Adenosine A_3 receptor stimulation and cerebral ischemia. *Eur. J. Pharmacol.* **1994**, *263*, 59−67.

(12) Colotta, V.; Cecchi, L.; Catarzi, D.; Filacchioni, G.; Martini, C.; Tacchi, P.; Lucacchini, A. Synthesis of some tricyclic heteroaromatic systems and their A_1 and A_{2a} adenosine binding activity. *Eur. J. Med. Chem.* **1995**, *30*, 133−139.

(13) Catarzi, D.; Cecchi, L.; Colotta, V.; Filacchioni, G.; Martini, C.; Tacchi, P.; Lucacchini, A. Tricyclic heteroaromatic systems. Synthesis and A_1 and A_{2a} adenosine binding activities of some 1-aryl-1,4-dihydro-3-methyl[1]benzopyrano[2,3-*c*]pyrazol-4-ones, 1-aryl-4,9-dihydro-3-methyl-1*H*-pyrazolo[3,4-*b*]quinolin-4-ones, and 1-aryl-1*H*-imidazo[4,5-*b*]quinoxalines. *J. Med. Chem.* **1995**, *38*, 1330−1336.

(14) Colotta, V.; Catarzi, D.; Varano, F.; Cecchi, L.; Filacchioni, G.; Martini, C.; Trincavelli, L.; Lucacchini, A. 4-Amino-6-benzylamino-1,2-dihydro-2-phenyl-1,2,4-triazolo[4,3*a*] quinoxalin-1-one: a new A_{2A} adenosine receptor antagonist with high selectivity versus A_1 receptors. *Arch. Pharm.* **1999**, *332*, 39−41.

(15) Colotta, V.; Catarzi, D.; Varano, F.; Cecchi, L.; Filacchioni, G.; Martini, C.; Trincavelli, L.; Lucacchini, A. Synthesis and structure−activity relationships of a new set of 2-arylpyrazolo[3,4-*c*]quinoline derivatives as adenosine receptor antagonists. *J. Med. Chem.* **2000**, *43*, 3118−3124.

(16) Colotta, V.; Catarzi, D.; Varano, F.; Cecchi, L.; Filacchioni, G.; Martini, C.; Trincavelli, L.; Lucacchini, A. 1,2,4-Triazolo[4,3-*a*]-quinoxalin-1-one: a versatile tool for the synthesis of potent and selective adenosine receptor antagonists. *J. Med. Chem.* **2000**, *43*, 1158−1164.

(17) Colotta, V.; Catarzi, D.; Varano, Filacchioni, G.; Martini, C.; Trincavelli, L.; Lucacchini, A. Synthesis and structure−activity relationships of a new set of 1,2,4-Triazolo[4,3-*a*]quinoxalin-1-one Derivatives as Adenosine Receptor Antagonists. *Bioorg. Med. Chem.* **2003**, *11*, 3541−3550.

(18) Colotta, V.; Catarzi, D.; Varano, F.; Cecchi, L.; Filacchioni, G.; Galli, A.; Costagli, C. Tricyclic heteroaromatic systems. 1,2,4-Triazolo[4,3-*a*]quinoxalines and 1,2,4-triazino[4,3-*a*]quinoxalines: synthesis and central benzodiazepine receptor activity. *Arch. Pharm.* **1997**, *330*, 387−391.

(19) Shawali, A. S.; Albar, H. A. Kinetics and mechanism of dehydrochlorination of *N*-aryl-*C*-ethoxycarbonylformohydrazidoyl chlorides. *Can. J. Chem.* **1986**, *64*, 871−875.

(20) Borovikov, Y. Y.; Lozinskii, M. O.; Kukota, S. N.; Pel'kis, P. S. Dipole moments of ethyl esters of arylhydrazonochloroglyoxalic acid. *Zh. Obsch. Khim.* **1972**, *42*, 687−692 [*Chem. Abstr.* **1972**, *77*, 53662].

(21) Lozinskii, M. O.; Kukota, S. N.; Pel'kis, P. S. Ethyl arylazochloroacetates and their reactions with morpholine and hydrazine hydrate. *Ukr. Khim. Zh.* **1967**, *33*, 1295−1296 [*Chem. Abstr.* **1968**, *69*, 51762].

(22) Salvatore, C. A.; Jacobson, M. A.; Taylor, H. E.; Linden, J.; Johnson, R. G. Molecular cloning and characterization of the human A_3 adenosine receptor. *Proc. Natl. Acad. Sci. U.S.A.* **1993**, *90*, 10365−10369.

(23) Klotz, K.-N. Adenosine receptors and their ligands. *Naunyn-Schmiedeberg's Arch. Pharmacol.* **2000**, *362*, 392−401.

(24) Lorenzen, A.; Guerra, L.; Vogt, H.; Schawabe, U. Interaction of full and partial agonists of the A_1 adenosine receptor with receptor/G protein complexes in rat-membranes. *Mol. Pharmacol.* **1996**, *49*, 915−926.

(25) Jacobson, K. A.; Park, K. S.; Jiang, J.-L.; Kim, Y.-C.; Olah, M. E.; Stiles, G. L.; Ji, X.-D. Pharmacological characterization of novel A_3 adenosine receptor-selective antagonists. *Neuropharmacology* **1997**, *49*, 915−926.

(26) (a) Müller, C. E. Medicinal Chemistry of adenosine A_3 receptor ligands. *Curr. Top. Med. Chem.* **2003**, *3*, 445−462. (b) Maconi, A.; Pastorin, G.; Da Ros, T.; Spalluto, G.; Gao, Z.-G.; Jacobson, K. A.; Baraldi, P. G.; Cacciari, B.; Varani, K.; Moro, S.; Borea, P. A. Synthesis, biological properties, and molecular modeling investigation of the first potent, selective, and water-soluble human A_3 adenosine receptor antagonist. *J. Med. Chem.* **2002**, *45*, 3579−3582.

(27) Klotz, K.-N.; Hessling, J.; Hegler, J.; Owman, C.; Kull, B.; Fredholm, B. B.; Lohes, M. J. Comparative pharmacology of human adenosine receptor subtypes-characterization of stably transfected receptors in CHO cells. *Naunyn-Schiedeberg's Arch. Pharmacol.* **1998**, *357*, 1−9.

(28) Baraldi, P. G.; Cacciari, B.; Moro, S.; Romagnoli, R.; Spalluto, G.; Pastorin, G.; Da Ros, T.; Klotz, K. N.; Leung, E.; Varani, K.; Gessi, S.; Merighi, S.; Borea, P. A. Synthesis, biological activity, and molecular modeling investigation of new pyrazolo[4,3-*e*]1,2,4-triazolo[1,5-*c*]pyrimidine derivatives as human A_3 adenosine receptor antagonists. *J. Med. Chem.* **2002**, *45*, 770−780.

(29) Pastorin, G.; Da Ros, T.; Spalluto, G.; Cacciari, B.; Moro, S.; Deflorian, F.; Varani, K.; Gessi, S.; Borea P. A. Pyrazolo[4,3-*e*]1,2,4-triazolo[1,5-*c*]pyrimidine derivatives as adenosine receptor antagonists: influence of the N5 substituent on the affinity at the human A_3 and A_{2B} adenosine receptor subtypes. *J. Med. Chem.* **2003**, *46*, 4287−4296.
(30) Moro, S.; Deflorian, F.; Spalluto, G.; Pastorin, G.; Cacciari, B.; Kim, S.-K.; Jacobson, K. A. Demystifying the Three Dimensional Structure of G Protein-Coupled Receptors with the Aid of Molecular Modeling. *J. Chem. Soc., Chem. Commun.* **2003**, 2949−2956.
(31) Palczewski, K.; Kumasaka, T.; Hori, T.; Behnke, C. A.; Motoshima, H.; Fox, B. A.; Le Trong, I.; Teller, D. C.; Okada, T.; Stenkamp, R. E.; Yamamoto, M.; Miyano, M. Crystal Structure of Rhodopsin: a G Protein-Coupled Receptor. *Science* **2000**, *289*, 739−745.
(32) Gao, Z. G.; Chen, A.; Barak, D.; Kim, S.-K.; Muller, C. E.; Jacobson, K. A. Identification by site-directed mutagenesis of residues involved in ligand recognition and activation of the human A3 adenosine receptor. *J. Biol. Chem.* **2002**, *277*, 19056−19063.
(33) Colotta, V.; Catarzi, D.; Varano, F.; Melani, F.; Filacchioni, G.; Cecchi, L.; Trincavelli, L.; Martini, C.; Lucacchini, A. Synthesis and A_1 and A_{2A} adenosine binding activity of some pyrano[2,3-*c*]pyrazol-4-ones. *Farmaco* **1998**, *53*, 189−196.
(34) Cheng, Y. C.; Prusoff, W. H. Relation between the inhibition constant K_i and the concentration of inhibitor which causes fifty percent inhibition (IC_{50}) of an enzyme reaction. *Biochem. Pharmacol.* **1973**, *22*, 3099−3108.
(35) Karton, Y.; Jiang, J. L.; Ji, X. D.; Melman, N.; Olah, M. E.; Stiles, G. L.; Jacobson, K. A. Synthesis and biological activities of flavonoid derivatives as A_3 adenosine receptor antagonists. *J. Med. Chem.* **1996**, *39*, 2293−2301.
(36) OpenMosix, http://www.openMosix.org.
(37) *Molecular Operating Environment* (MOE 2003.02); Chemical Computing Group, Inc. (1255 University Street, Suite 1600, Montreal, Quebec, Canada, H3B 3X3), 2003.
(38) *Spartan O2*; Wavefuncion Inc. (18401 Von Karman Avenue, Irvine, CA 92612).
(39) Cornell, W. D.; Cieplak, P.; Bayly, C. I.; Gould, I. R.; Merz, K. M.; Ferguson, D. M.; Spellmeyer, D. C.; Fox, T.; Caldwell, J. W.; Kollman, P. A. A Second Generation Force Field for the Simulation of Proteins, Nucleic Acids and Organic Molecules. *J. Am. Chem. Soc.* **1995**, *117*, 5179−5196.
(40) Baxter, C. A.; Murray, C. W.; Clark, D. E.; Westhead, D. R.; Eldridge, M. D. Flexible Docking Using Tabu Search and an Empirical Estimate of Binding Affinity. *Proteins: Struct., Funct., Genet.* **1998**, *33*, 367−382.
(41) Halgren, T. A. Merck Molecular Force Field. I. Basis, Form, Scope, Parameterization, and Performance of MMFF94. *J. Comput. Chem.* **1996**, *17*, 490−519.
(42) Halgren, T. A. Merck Molecular Force Field. II. MMFF94 van der Waals and Electrostatic Parameters for Intermolecular Interactions. *J. Comput. Chem.* **1996**, *17*, 520−552.
(43) Halgren, T. A. Merck Molecular Force Field. III. Molecular Geometries and Vibrational Frequencies for MMFF94. *J. Comput. Chem.* **1996**, *17*, 553−586.
(44) Halgren, T. A. Merck Molecular Force Field. IV. Conformational Energies and Geometries for MMFF94. *J. Comput. Chem.* **1996**, *17*, 587−615.
(45) Halgren, T. A.; Nachbar, R. Merck Molecular Force Field. V. Extension of MMFF94 Using Experimental Data, Additional Computational Data, and Empirical Rules. *J. Comput. Chem.* **1996**, *17*, 616−641.
(46) Halgren, T. A. MMFF. VI. MMFF94s Option for Energy Minimization Studies. *J. Comput Chem.* **1999**, *20*, 720−729.
(47) Halgren, T. A. MMFF. VII. Characterization of MMFF94, MMFF94s, and Other Widely Available Force Fields for Conformational Energies and for Intermolecular-Interaction Energies and Geometries. *J. Comput Chem.* **1999**, *20*, 730−748.

JM031136L